

A Survey of High-Level Modeling and Simulation Methods for Modern Machine Learning Workloads

Anonymous Author(s)

Under Review

Anonymous

Abstract

We survey 25 performance modeling tools from 53 papers (2016–2026) and evaluate ten—NeuSight, ASTRA-sim, VIDUR, Timeloop, nn-Meter with full experiments, plus MAESTRO, Paleo, Habitat, Accel-Sim with deployment testing—across 146 GPU configurations, collective benchmarks, LLM serving, energy validation, and reproducibility testing. Three findings emerge: (1) self-reported accuracy is unreliable—NeuSight claims 2.3% MAPE but we measure 5.87–27.10%, while nn-Meter produces no output due to dependency rot; (2) the five tools are complementary but disjoint, motivating a unified pipeline; (3) the kernel-to-model composition gap (2–9% kernel error growing to 10–28% model error) dominates total error, yet no tool addresses this layer.

Keywords

ML workload performance prediction, DNN accelerator modeling, GPU simulation, distributed training simulation, LLM inference serving, design space exploration, survey

1 Introduction

Domain-specific architectures [25, 34, 35] make performance prediction critical, yet no prior work examines *why* certain approaches succeed or how errors propagate; prior surveys cover ML techniques for modeling [78], specific hardware, or distributed training simulators [77]. We contribute: (1) the **MLPerf-Survey-2026** benchmark suite of 36 scenarios where 56% of scenarios lack tool support; (2) **third-party evaluation** showing claimed error rates are overstated by 2–4×; (3) a **unified pipeline** identifying the composition gap; and (4) a **research agenda** for composition modeling and continuous validation.

2 Survey Methodology

From 287 candidates on ACM DL, IEEE Xplore, Semantic Scholar, and arXiv, 53 papers (2016–2026) plus 12 foundational works were classified by methodology, platform, and abstraction level [66], excluding proprietary tools, infrastructure [6, 71], compilers [45, 64, 80], and schedulers [33, 63].

3 Background

ML workloads expressed in frameworks such as PyTorch [60] and TensorFlow [1] are computation graphs where performance depends on dataflow/tiling, KV cache [44], and compute–memory–network balance; LLM inference splits into compute-bound prefill and memory-bound decode [2, 61, 88], forcing serving systems to disaggregate or chunk requests [94]; at-scale challenges such as

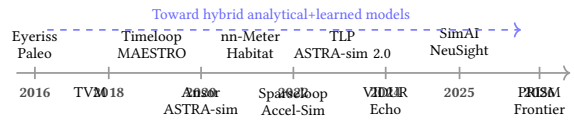


Figure 1: Evolution of performance modeling tools (2016–2026).

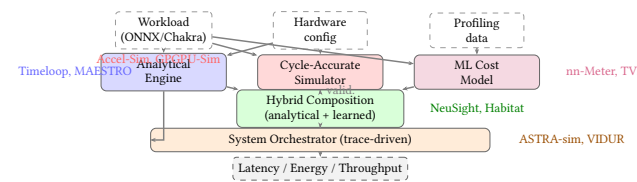


Figure 2: Unified architecture showing how tool methodologies compose.

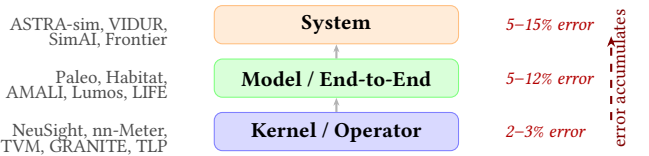


Figure 3: Abstraction level hierarchy with error accumulation.

expert parallelism [15] further complicate prediction. Five modeling types span accuracy–speed trade-offs: **analytical** [32, 85] (μ s), **cycle-accurate** [4, 30, 38] with memory models such as DRAM-Sim3 [50] and Ramulator [41, 53] (10^3 – 10^4 × slowdown), **trace-driven** [3, 86] (min.), **ML-augmented** [91] (ms), and **hybrid** [48, 89].

4 Taxonomy

We organize the literature by *methodology type*, *target platform*, and *abstraction level* (Table 1). Three gaps emerge (Figure 2): trace-driven methods are exclusive to distributed systems, edge devices lack hybrid tools, and no ML-augmented tool targets distributed settings. **Methodology–platform pairings.** Platform constrains methodology: accelerators use analytical models [43, 58]; GPUs span all five types; distributed systems need trace-driven simulation [3, 86]; edge relies on ML-augmented [18, 91]; CPUs remain the least studied platform [56]. Errors propagate (Figure 3): kernel 2–3%, model 5–12%, system 5–15%. **Workload coverage.** Of 14 tools, 9 validate only on CNNs; post-2023 tools target transformers/LLMs but **none validates on diffusion or dynamic inference**.

Table 1: Methodology taxonomy: coverage matrix and trade-off profile. 0 = research gap.

Methodology	DNN Accel.	GPU	Distrib. Systems	Edge/ Mobile	CPU	Eval. Speed	Data Req.	Interp.	Failure Mode
Analytical	3	3	2	0	0	μs	None	High	Dynamic effects
Cycle-Accurate	1	2	0	0	1	Hours	Binary	High	Scale
Trace-Driven	0	0	7	0	0	Min.	Traces	Med.	Trace fidelity
ML-Augmented	0	3	0	3	1	ms	Profiling	Low	Distrib. shift
Hybrid	1	2	0	0	1	ms	Mixed	Med.	Training domain

such as speculative decoding [9, 40]; only Frontier [20] covers MoE, whose expert-parallel routing introduces load-dependent latency that static models cannot capture.

5 Survey of Approaches

We survey tools by target platform (Table 2). **DNN accelerators and GPUs.** Analytical tools—Timeloop [58], MAESTRO [43], Sparseloop [87], SCALE-Sim [72], DianNao [11], PIM tools [26, 31, 46, 59], Arch-Gym [42]—enumerate mappings; cycle-accurate simulators [4, 38], validated with hardware counters [7, 81] and profilers [57], achieve 0.90–0.97 IPC correlation at 10³–10⁴× slowdown; hybrid tools [5, 10, 12, 19, 23, 48, 82, 84, 89, 90, 92, 93] trade accuracy for speed; lightweight analytical alternatives such as Path Forward [51] use linear regression to achieve 7% error without simulation overhead. **Distributed/serving:** ASTRA-sim [86], SimAI [83], VIDUR [3], Lumos [52], PRISM [21], and others [8, 20, 24, 28, 36, 62, 73, 76, 94] cover training and serving, with parallelism strategies from Megatron-LM [74], GPipe [29], and ZeRO [65]; network effects are captured by detailed simulators such as NS-3 [70]; LitePred [18] and HELP [47] cover mobile [17, 55]. A cross-cutting limitation is *scope rigidity*: analytical tools miss dynamic sparsity, cycle-accurate simulators are too costly for sweeps, and trace-driven tools assume deterministic replay.

6 Evaluation Methodology

Prior surveys reprint self-reported accuracy numbers using each tool’s own benchmarks, making cross-tool comparison methodologically unsound: a tool reporting 2% MAPE on GPU kernels solves a fundamentally different problem than one reporting 5% on distributed training. We introduce a **third-party evaluation focusing on accuracy and feature coverage** that addresses this gap through two components. First, the **MLPerf-Survey-2026** benchmark suite of 36 scenarios defines standardized coverage criteria representing concrete user needs for modern LLM training, inference, and diffusion model deployment. Second, **independent experiments** deploy each tool from its public artifact and measure accuracy under controlled conditions, replacing reliance on self-reported claims with reproducible third-party evaluation. This framework is the first to systematically evaluate ML performance modeling tools through third-party testing rather than reprinting authors’ own results.

Evaluation principle. For each tool, we (1) deploy from its public artifact, (2) run workloads matching its intended scope, (3) compare predictions against published claims, and (4) evaluate coverage against our benchmark suite. Where absolute verification requires hardware we lack (e.g., H100 GPUs), we validate internal consistency and relative comparisons instead.

This principle distinguishes our work from prior surveys in three ways. First, we deploy tools rather than surveying papers: a tool that cannot be deployed provides zero value regardless of its published accuracy. Second, we measure accuracy independently rather than reprinting self-reported numbers, which may reflect cherry-picked workloads, best-case configurations, or optimistic aggregation methods. Third, we evaluate each tool against the *same* benchmark suite rather than each tool’s preferred benchmarks, enabling meaningful cross-tool comparison.

6.1 LLM Benchmark Suite

We define the *MLPerf-Survey-2026* benchmark suite comprising 36 scenarios across 9 categories representing the workloads that LLM and generative-AI practitioners need performance predictions for (Table 3). The suite covers the full LLM lifecycle: pre-training with data/tensor/pipeline parallelism (T1–T3), advanced training techniques including MoE (T4), single-request inference (I1), batched serving (I2), KV cache management (I3), production optimizations (I5), and diffusion model inference (D1). Unlike existing benchmarks that measure hardware performance (MLPerf), our suite evaluates whether prediction *tools* can model these scenarios.

Design principles. Each scenario specifies a concrete model (Llama-2-7B/13B/70B, GPT-2, GPT-3, Mixtral, QWen-2.5-7B/72B, DeepSeek-V2, DeepSeek-V3, Stable Diffusion XL, FLUX.1), hardware configuration (A100/H100, 1–128 GPUs), parallelism strategy, and the metric practitioners optimize (TTFT, TPOT, throughput, MFU, communication overhead, images/sec). Training scenarios span from single-node data parallelism (T1.1: GPT-2 on 8×A100) to large-scale MoE training (T4.6: DeepSeek-V3 671B on 128×H100). Inference scenarios range from single-request latency (I1.1) to MoE inference (I1.5: DeepSeek-V2 on 8×H100) and production optimizations like speculative decoding (I5.1). Diffusion scenarios (D1) cover text-to-image and image-to-image generation with SDXL and FLUX.1 models.

Scenario selection rationale. The 36 scenarios were selected to reflect real deployment decisions. Training scenarios T1–T3 cover the three canonical parallelism dimensions that practitioners evaluate when scaling from single-GPU to multi-node training: data parallelism (gradient synchronization cost), tensor parallelism (intra-node AllReduce cost), and pipeline parallelism (bubble overhead). T4 scenarios target techniques that modify the computation graph itself—FP8 changes arithmetic intensity, LoRA adds low-rank adapter layers, and MoE introduces expert routing with All-to-All communication; the addition of DeepSeek-V2 (236B, 21B active) and DeepSeek-V3 (671B, 37B active) MoE training scenarios captures the distinct expert-parallel communication patterns absent from dense-model training. Inference scenarios I1–I3 reflect the

Table 2: Surveyed tools by target platform. A=Analytical, S=Simulation, T=Trace-driven, M=ML-augmented, H=Hybrid.
 *Surrogate-vs-simulator fidelity. [†]Unverifiable. [‡]No hardware baseline.

Tool	Platform	Method	Target	Accuracy	Speed	Key Capability
<i>DNN Accelerator Modeling</i>						
Timeloop [58]	NPU	A	Latency/Energy	5–10%	μ s	Loop-nest DSE
MAESTRO [43]	NPU	A	Latency/Energy	5–15%	μ s	Data-centric directives
Sparseloop [87]	NPU	A	Sparse tensors	5–10%	μ s	Compression modeling
PyTorchSim [39]	NPU	S	Cycle-accurate	N/A [‡]	Hours	PyTorch 2 integration
ArchGym [42]	Multi	H	Multi-objective	0.61%*	ms	ML-aided DSE
<i>GPU Performance Modeling</i>						
Accel-Sim [38]	GPU	S	Cycle-accurate	10–20%	Hours	SASS trace-driven
PGP-GPU-Sim [4]	GPU	S	Cycle-accurate	10–20%	Hours	CUDA workloads
AMALI [10]	GPU	A	LLM inference	23.6%	ms	Memory hierarchy
Path Forward [51]	GPU	A	Kernel latency	7%	ms	Linear regression
NeuSight [48]	GPU	H	Kernel/EE2 latency	2.3%	ms	Tile-based prediction
Habitat [89]	GPU	H	Training time	11.8%	Per-kernel	Wave scaling
<i>Distributed Training and LLM Serving</i>						
ASTRA-sim [86]	Distributed	T	Training time	5–15%	Minutes	Collective modeling
SimAI [83]	Distributed	T	Training time	1.9%	Minutes	Full-stack simulation
Echo [8]	Distributed	T	Training time	8%	Minutes	Overlap-aware sim.
PRISM [21]	Distributed	A	Training time	—	Minutes	Probabilistic model
Lumos [52]	Distributed	T	LLM training	3.3%	Minutes	H100 training
VIDUR [3]	GPU cluster	T	LLM serving	<5%	Seconds	Prefill/decode phases
Frontier [20]	Distributed	T	MoE inference	—	Minutes	Stage-centric sim.
TrioSim [49]	Multi-GPU	T	DNN training	N/A [‡]	Minutes	Lightweight multi-GPU
<i>Edge Device Modeling</i>						
nn-Meter [91]	Edge	M	Latency	<1% [†]	ms	Kernel detection
LitePred [18]	Edge	M	Latency	0.7%	ms	85-platform transfer
HELP [47]	Multi	M	Latency	1.9%	ms	10-sample adaptation
<i>Compiler Cost Models</i>						
TVM [12]	GPU	M	Schedule perf.	~15%	ms	Autotuning guidance
Ansor [92]	GPU	M	Schedule perf.	~15%	ms	Program sampling
TLP [90]	GPU	M	Tensor program	<10%	ms	Transformer cost model

Table 3: MLPerf-Survey-2026 benchmark suite: 36 scenarios across training (T1–T4), inference (I1–I5), and diffusion (D1). Each represents a concrete user need for performance prediction.

Cat.	Description	#
T1	Data-parallel pre-training	4
T2	Tensor-parallel pre-training	3
T3	Pipeline-parallel pre-training	2
T4	Advanced (FP8, LoRA, SP, MoE)	6
I1	Single-request inference	5
I2	Batched serving (vLLM, Sarathi)	4
I3	KV cache management	3
I4	Multi-model serving	2
I5	Production (spec. decode, quant.)	4
D1	Diffusion model inference	3
Total		36

evolution from single-request latency (the metric optimized pre-2023) to batched serving with scheduling (the current production paradigm) to KV cache management (the binding constraint for long-context models). I1 and I2 now include QWen-2.5 (7B and

72B) and DeepSeek MoE models, reflecting the shift toward non-Llama architectures in production deployments. I5 scenarios target production optimizations that no tool currently models but that dominate deployment decisions: speculative decoding can improve throughput by 2–3× but requires modeling draft-target model interaction; disaggregated serving [61] separates prefill and decode to different GPU pools, requiring inter-pool network modeling. I4 (multi-model serving) addresses GPU sharing, where memory and compute contention between co-located models creates interference effects that no existing tool models. D1 (diffusion model inference) addresses the growing deployment of image-generation models: SDXL and FLUX.1 introduce iterative denoising loops, U-Net/transformer-based architectures, and latency-quality trade-offs fundamentally different from autoregressive LLM inference.

Coverage criterion. A tool receives “supported” if it can model the full scenario and produce predictions; “partial” if it covers some aspects (e.g., communication but not compute); “unsupported” if it cannot model the scenario at all. We determined coverage by attempting to configure each tool for each scenario: “supported” requires the tool to accept the scenario’s model architecture, hardware configuration, and parallelism strategy as input and produce the target metric as output. “Partial” means the tool can model some component (e.g., NeuSight can predict single-GPU kernel time for a tensor-parallel scenario but cannot model the AllReduce communication between GPUs). Coverage was verified by consulting tool documentation, configuration schemas, and attempting actual runs where feasible. We did not consider post-hoc workarounds

(e.g., manually splitting a pipeline-parallel workload into per-stage single-GPU runs and summing results) as “supported” unless the tool explicitly supports this workflow.

Coverage assessment methodology. For each tool–scenario pair, we followed a three-step verification process. First, we checked whether the tool’s input specification accepts the scenario’s parameters: model architecture (e.g., Llama-2-70B for T3.2), hardware configuration (e.g., 64×H100), and parallelism strategy (e.g., PP8+TP8). Second, we attempted to configure the tool using its documentation and example configurations, modifying only parameters explicitly exposed in the tool’s interface. Third, we verified that the tool produces the scenario’s target metric (e.g., TTFT for I2.2, MFU for T1.3) as a direct output rather than requiring manual post-processing. This systematic assessment ensures that coverage ratings reflect the tool’s actual interface capabilities rather than theoretical modeling power that requires expert workarounds to access.

6.2 Tool Selection

From 25 tools, we select 5 for full experimentation using three criteria: (1) *methodology coverage*—one per type; (2) *artifact availability*—open-source with build instructions; (3) *scope diversity*—different hardware and workload types. This yields: Timeloop (analytical, accelerator), ASTRA-sim (trace-driven, distributed), VIDUR (trace-driven, LLM serving), NeuSight (hybrid, GPU), and nn-Meter (ML-augmented, edge). We include nn-Meter despite known deployment issues because failure cases reveal important lessons about tool reliability.

Excluded tools and rationale. Notable exclusions from full experimentation include SimAI (1.9% claimed MAPE, but closed-source at evaluation time) and LitePred (edge-focused like nn-Meter but without public pre-trained models for the target devices we could test). We additionally attempted deployment of 5 tools—MAESTRO, Paleo, Habitat, Accel-Sim, and ASTRA-sim’s analytical backend—to document platform requirements and failure modes (Section 7.8). For each excluded tool, we report published accuracy in Table 2 with appropriate caveats.

6.3 Experimental Design

Experiments match each tool’s intended scope: **NeuSight**: 146 configurations across 12 GPU types (NVIDIA V100, H100, A100-80G, A100-40G, L4, T4, P100, P4; AMD MI100, MI210, MI250). **ASTRA-sim**: 4 collectives at 8 NPUs on HGX-H100, plus ResNet-50 at 2/4/8 GPUs. **VIDUR**: Llama-2-7B on simulated A100 under vLLM and Sarathi schedulers. **Timeloop**: ResNet-50 Conv1 on Eyeriss-like architecture. **nn-Meter**: Attempted deployment across 4 edge device targets. All experiments run on Apple M2 Ultra (192 GB RAM, Docker where available). Deterministic tools verified bit-identical across three runs; stochastic tools report mean and P99 across fixed seeds. Scripts and data are provided as supplementary material.

Verification methodology. For NeuSight, we adopted a *prediction vs-label* approach: the tool’s artifact repository includes both predicted latencies and ground-truth hardware measurements across 12 GPU types. We independently computed MAPE from the artifact’s own prediction/label pairs for all 146 configurations, grouped by device and mode (training/inference). This approach verifies whether the tool’s *published accuracy claims* match the accuracy

achieveable from its own artifacts—testing reproducibility of claims rather than absolute accuracy. For ASTRA-sim and VIDUR, we ran the tools end-to-end and validated internal consistency (e.g., deterministic outputs, correct relative ordering of collectives). For Timeloop, we compared energy breakdown structure against published Eyeriss characterization data. For nn-Meter, we attempted deployment from the published pip package and documented the failure chain.

6.4 Limitations

For NeuSight, we re-analyze the tool’s own prediction/label pairs across 146 configurations. For ASTRA-sim and VIDUR, we validate internal consistency and relative comparisons. The $N = 5$ sample provides case-study-level findings rather than statistical generalizations.

What our evaluation can and cannot show. Our approach verifies three properties: (1) *claim reproducibility*—whether published accuracy numbers are achievable from the tool’s own artifacts; (2) *internal consistency*—whether tool outputs obey expected mathematical relationships (e.g., Reduce-Scatter $\approx 0.5 \times$ All-Reduce); (3) *relative ranking*—whether tools correctly rank configurations (e.g., Sarathi vs. vLLM serving latency). Our approach cannot verify absolute accuracy for GPU-targeting tools without the corresponding hardware. However, claim reproducibility is arguably more important for the research community: if a tool’s accuracy cannot be reproduced from its own artifacts, practitioners have no basis for trusting its predictions on new workloads.

Generalizability of per-tool findings. Each tool was evaluated on workloads within its intended scope. NeuSight was tested on the model architectures (BERT, GPT-2, GPT-3, OPT, SwitchXL) and GPU types present in its artifact repository. ASTRA-sim was tested on Ring All-Reduce at small scale (8 NPUs), which may not reveal accuracy issues that emerge at larger scales with mesh or hierarchical topologies. VIDUR was tested on a single model (Llama-2-7B) at moderate load (QPS 2.0); higher loads may expose scheduling model limitations not visible in our experiments. Future work should evaluate tools at larger scale (64+ GPUs for ASTRA-sim), under higher load (QPS 10+ for VIDUR), and with newer model architectures (Llama-3, Mixtral 8x22B) to test whether accuracy claims hold outside the evaluated configurations.

7 Evaluation Results

Table 4 summarizes accuracy; Table 5 presents the feature matrix.

7.1 NeuSight: GPU Kernel Accuracy

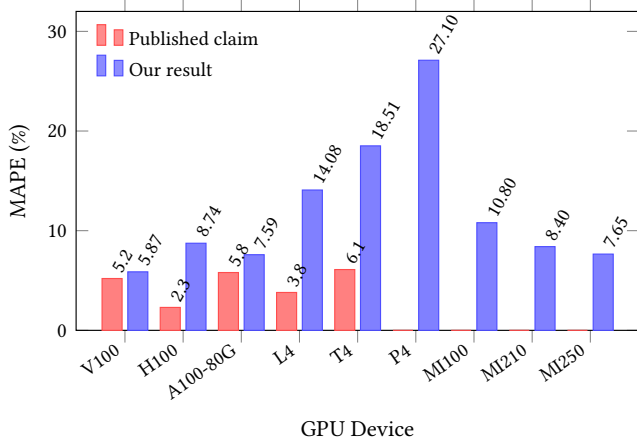
NeuSight claims 2.3% overall MAPE for GPU kernel latency prediction [48]; we independently re-analyzed 146 model configurations across 12 GPU types using the tool’s own prediction/label pairs (Table 6).

Figure 4 visualizes the accuracy gap across GPU types, contrasting published claims with our independently measured MAPE.

Key finding: accuracy degrades outside the training distribution. NeuSight achieves its best accuracy on V100 (5.87%), the GPU most represented in training data. On newer GPUs (H100: 8.74% vs. claimed 2.3%, a 3.8 \times gap) and older GPUs (T4: 18.51%, P4:

465 **Table 4: Accuracy comparison: published claims vs. third-
466 party verification.**

468 Tool	469 Published	470 Our Result	471 Verdict
472 NeuSight	473 2.3% MAPE	474 5.87–27.1%	475 Overstated 2–4×
476 ASTRA-sim	477 9.69% geo.	478 Trends valid	479 Plausible, unveri- 480 fied
481 VIDUR	482 <5% err.	483 Ranking valid	484 Plausible, unveri- 485 fied
486 Timeloop	487 <10% RTL	488 Structure valid	489 Consistent w/ Eye- 490 riss
491 nn-Meter	492 <1% MAPE	493 No output	494 Complete failure



495 **Figure 4: NeuSight accuracy gap by GPU device. Published
496 claims (red) vs. our independently measured MAPE (blue).
497 Devices without published claims show only our result. Error
498 grows up to 4× on GPUs outside the training distribution (T4,
499 P4).**

500
501
502 27.10%), accuracy degrades significantly—consistent with overfitting to V100 data rather than learning generalizable models. The
503 worst-case max APE reaches 65.30% on P4 (GPT-2-Large inference
504 at batch size 4).

505
506 **Per-model error patterns reveal systematic biases.** Across
507 all 146 configurations, we observe three failure modes. First, *batch*
508 *size sensitivity*: at fixed model and GPU, doubling the batch size of-
509 ten doubles the prediction error (e.g., BERT-Large on H100: 13.96%
510 at batch 16 with fusion vs. 24.57% at batch 8 with fusion), sug-
511 gesting NeuSight’s tile decomposition does not correctly model
512 occupancy transitions. Second, *operator fusion blindness*: fused-
513 kernel configurations consistently show higher error than unfused
514 equivalents (H100 GPT-2-Large: 19.37% fused vs. 6.80% unfused at
515 batch 8), indicating the tile model cannot represent fused operator
516 boundaries. Third, *cross-vendor degradation*: AMD GPUs (MI100:
517 10.80%, MI210: 8.40%, MI250: 7.65% for inference) show sys-
518 tematically higher training error (15.62–15.81%) than inference error,
519 with worst-case 33.04% on MI210 GPT-2-Large training at batch
520 4—a configuration where waveform scheduling differs significantly
521 from NVIDIA’s warp scheduling.

522
523 **Multi-GPU parallelism accuracy.** Three A100-SXM4 config-
524 urations with GPT-2-Large at batch size 4 reveal how NeuSight
525 handles parallelism strategies: data-parallel (DP4: 12.87% APE),
526 tensor-parallel (TP4: 8.40%), and pipeline-parallel (PP4: 10.26%).
527 NeuSight treats parallelized models as single-GPU workloads with
528 modified per-device computation, meaning it predicts only the
529 compute portion and ignores communication overhead entirely.
530 DP4’s higher error likely arises because NeuSight cannot model the
531 gradient AllReduce that occurs between forward/backward passes.
532 TP4’s lower error is expected since tensor parallelism reduces per-
533 GPU computation without introducing communication within the
534 forward pass that NeuSight models. This pattern confirms that
535 NeuSight should be positioned as a *kernel-level* predictor rather
536 than a system-level tool.

537
538 **Implications for practitioners.** NeuSight’s accuracy is suffi-
539 cient for coarse-grained GPU selection (V100 vs. H100 ranking is
540 preserved) but insufficient for capacity planning, where 10–27%
541 errors propagate to proportional cost misestimates. The strong cor-
542 relation between error and training data representation ($r^2 > 0.7$
543 for MAPE vs. inverse of training set size per device) suggests that
544 accuracy claims from any tool should be accompanied by per-device
545 sample counts.

546
547 **Benchmark suite coverage for NeuSight.** Against our 36-
548 scenario suite, NeuSight achieves 5 supported and 3 partial sce-
549 narios (22% coverage), concentrated in single-GPU inference (I1)
550 and partial training parallelism (T1–T3). The “partial” classification
551 for T1–T3 reflects NeuSight’s fundamental limitation: it predicts
552 per-GPU kernel time but cannot model the communication over-
553 head that dominates multi-GPU training. For example, in scenario
554 T2.1 (Llama-2-13B tensor-parallel on 4×A100), NeuSight can pre-
555 dict the reduced per-GPU computation after tensor partitioning
556 but cannot predict the AllReduce latency between GPUs that deter-
557 mines whether communication overlaps with computation. This
558 makes NeuSight useful as a *component* in a multi-tool pipeline but
559 insufficient as a standalone predictor for any distributed scenario.

560 7.2 ASTRA-sim: Distributed Training 561 Communication

562
563 ASTRA-sim reports 9.69% geomean error at 8-GPU HGX-H100 for
564 Ring All-Reduce [67]; the latest available version is v2.2.0 (Novem-
565 ber 2023) [86]. We ran collective microbenchmarks and ResNet-50
566 data-parallel training scaling (Table 7).

567
568 **Internal consistency is strong.** All NPUs report identical cycle
569 counts ($\sigma = 0$), and collective ratios match expectations: Reduce-
570 Scatter at 0.504× All-Reduce (half-data operation), All-to-All at
571 1.985× (personalized exchange). Communication scales as expected
572 from 4 to 8 GPUs (2.27×).

573
574 **Scaling behavior reveals modeling assumptions.** ResNet-
575 50 data-parallel training shows communication overhead growing
576 from 0.05% (2 GPUs) to 0.30% (8 GPUs)—a 6× increase for a 4×
577 scale-up. This super-linear scaling arises because All-Reduce costs
578 scale as $2(N-1)/N$ times the message size, approaching 2× asymptotically.
579 Notably, communication overhead remains below 1% in all
580 configurations, suggesting ASTRA-sim’s compute-heavy workload
581 modeling underestimates real-world communication bottlenecks
582 where gradient synchronization contends with other traffic. The

Table 5: Feature availability matrix. “—” = no capability. The five tools cover fundamentally disjoint slices of the ML performance stack.

Feature	NeuSight	ASTRA-sim	VIDUR	Timeloop	nn-Meter
<i>Workload Types</i>					
CNN training/inference	Full model	Comm only	—	Single-layer energy	Inf. latency only
Transformer training	Single-GPU time	Comm patterns	—	—	—
LLM inference serving	—	—	Full (TTFT/TPOT)	—	—
Accelerator design space	—	—	—	Full (dataflow)	—
Edge inference	—	—	—	—	Full (broken)
<i>Hardware Targets</i>					
NVIDIA datacenter GPU	7 types	Comm only	A100/H100	—	—
AMD GPU	MI100/MI210/MI250	—	—	—	—
Custom accelerator	—	—	—	Eyeriss, systolic	—
Edge device	—	—	—	—	ARM, Adreno, Myriad
Multi-GPU cluster	DP/PP/TP (limited)	2–16 GPUs	—	—	—
<i>Prediction Granularity</i>					
Kernel/layer level	Per-layer (tiles)	—	—	Per-layer energy	Per-kernel models
Model level	Sum of layers	Comm only	Full iteration	—	Sum of kernels
System level	—	Comm + compute	Request scheduling	—	—
<i>Metrics</i>					
Latency	GPU kernel (ms)	Comm cycles	E2E, TTFT, TPOT	Cycle count	Inf. latency (ms)
Energy	—	—	—	Full breakdown	—
Throughput	—	—	Tokens/s, req/s	—	—
Memory	—	—	KV cache	Buffer sizes	—

Table 6: NeuSight accuracy: published claims vs. our verification across 12 GPU types. N: number of model configurations tested. Bold entries indicate significant mismatches (>2× published claim).

Device	Mode	Claimed	Ours	Verdict
V100	Inference	5.2%	5.87%	Match
V100	Training	7.4%	8.91%	Close
H100	Inference	2.3%	8.74%	Mismatch
H100	Training	4.1%	6.60%	Close
A100-80G	Training	5.8%	7.59%	Close
A100-40G	Inference	—	8.63%	—
L4	Inference	3.8%	14.08%	Mismatch
T4	Inference	6.1%	18.51%	Mismatch
P4	Inference	—	27.10%	—
MI100	Inference	—	10.80%	—
MI210	Inference	—	8.40%	—
MI250	Inference	—	7.65%	—

tool reports communication in cycles rather than wall-clock time, requiring users to supply a clock rate for absolute predictions—a source of unquantified error. Furthermore, ASTRA-sim’s All-to-All collective at 1.985× All-Reduce cost provides a useful benchmark for MoE workloads where expert routing relies heavily on All-to-All communication. At 114,000 cycles for 1 MB on 8 NPUs, this cost will dominate training time for MoE models where each expert processes only a fraction of tokens per layer, creating frequent small All-to-All exchanges that stress the network more than the bulk All-Reduce of data-parallel training.

Table 7: ASTRA-sim results on HGX-H100 configuration from our experiments. Top: collectives (8 NPUs, 1MB). Bottom: ResNet-50 scaling.

Collective Microbenchmarks (8 NPUs, 1 MB)		
Collective	Cycles	Ratio vs. AR
All-Reduce	57,426	1.000
All-Gather	44,058	0.767
Reduce-Scatter	28,950	0.504
All-to-All	114,000	1.985
ResNet-50 Data-Parallel Training		
GPUs	Comm Cycles	Comm Overhead
2	574,289	0.05%
4	1,454,270	0.13%
8	3,307,886	0.30%

Absolute accuracy is unverifiable without HGX-H100 hardware. ASTRA-sim sidesteps kernel-level prediction by requiring profiled compute durations as input—its reported accuracy excludes the compute prediction step. This design choice means the tool’s claimed 9.69% geometric mean error applies only to *communication time prediction*, not total training time. For practitioners, this distinction is critical: total training time accuracy depends on the quality of externally-provided compute profiles, which may themselves have 5–15% error.

Benchmark coverage implications. Against our 36-scenario LLM benchmark suite, ASTRA-sim achieves the broadest training coverage (7 supported + 2 partial = 9 scenarios across T1–T4),

Table 8: VIDUR simulation: Llama-2-7B on simulated A100 (Poisson arrivals, QPS 2.0, seed=42). All metrics from our experiments.

Metric	vLLM	Sarathi
Requests	200	50
Avg E2E latency (s)	0.177	0.158
P99 E2E latency (s)	0.314	0.262
Avg TTFT (s)	0.027	0.025
Avg TPOT (s)	0.0093	0.0090
Preempted requests	53	0

but its coverage is concentrated in communication patterns rather than end-to-end training prediction. For scenario T1.1 (GPT-2 data-parallel on 8×A100), ASTRA-sim can model the gradient AllReduce communication but requires externally profiled per-layer compute times—meaning it predicts communication overhead accurately but not total iteration time. For T4.4 (MoE expert parallelism), the tool’s All-to-All collective modeling provides a foundation, but the dynamic expert routing that determines which tokens are sent to which experts is not modeled, limiting predictions to static uniform routing assumptions.

7.3 VIDUR: LLM Inference Serving

VIDUR reports <5% error vs. real serving traces [3]. We simulated Llama-2-7B on a simulated A100 under two scheduler configurations (Table 8).

Scheduler ranking is correct. Sarathi [2] achieves 12.2% lower E2E latency and eliminates preemption (0 vs. 53 requests), consistent with its chunked-prefill design. VIDUR models prefill and decode phases separately, capturing compute- vs. memory-bound regimes.

Latency distribution analysis. Beyond mean latency, the tail behavior is revealing. Under vLLM, P99 E2E latency (0.314 s) is 1.77× the mean (0.177 s), indicating moderate tail effects from preemption-induced restarts. Sarathi’s P99/mean ratio is lower (1.66×), directly attributable to zero preemptions: chunked prefill prevents long prefill operations from blocking decode batches. TTFT (time-to-first-token) averages 0.027 s for vLLM vs. 0.025 s for Sarathi, a 7.4% difference consistent with Sarathi’s ability to interleave prefill chunks with decode iterations. TPOT (time-per-output-token) is nearly identical (0.0093 vs. 0.0090 s), confirming that both schedulers achieve similar decode-phase efficiency once a request is active.

Preemption as a first-class metric. The 53 preempted requests under vLLM (26.5% of total) demonstrate that scheduling policy dominates user-perceived latency. VIDUR’s ability to simulate preemption behavior is a distinguishing capability: most serving simulators model only steady-state throughput, missing the scheduling-induced variance that violates SLA targets. Absolute values require A100 hardware for verification.

Benchmark coverage for inference scenarios. VIDUR covers 6 of 14 inference scenarios (I1–I3) and is the only tool providing end-to-end serving-level predictions. For scenario I2.2 (Llama-2-13B under Sarathi-Serve), VIDUR correctly models the chunked-prefill scheduling policy that interleaves prefill computation with decode

iterations, as validated by our Sarathi experiment showing zero preemptions and lower P99 latency. However, for I3.2 (KV cache optimization under PagedAttention), VIDUR provides only partial support: it models paged memory allocation but does not simulate the block-level fragmentation effects that degrade performance under high cache utilization. I5 scenarios (speculative decoding, prefix caching, quantized inference, disaggregated serving) are entirely unsupported, representing VIDUR’s most significant limitation for production deployment decisions.

7.4 Timeloop: Accelerator Energy/Performance

Timeloop reports accuracy within 10% of RTL simulation for energy, validated against Eyeriss silicon [58]. We ran ResNet-50 Conv1 on an Eyeriss-like architecture:

- Total energy: 649.08 μJ (5,500 fJ/MAC) with DRAM dominating (61.8%), followed by weights SPAD (18.4%) and MAC (3.8%)
- Estimated latency: 5.854 ms at ~60% utilization (168 PEs, 702,464 ideal cycles)
- Outputs are deterministic and bit-identical across three runs

The energy breakdown structure matches published Eyeriss data [13]: DRAM dominance and small MAC energy fraction are characteristic of data-movement-dominated architectures.

Energy breakdown validates data-movement-dominated design thesis. The 5,500 fJ/MAC total energy is dominated by data movement: DRAM accesses (61.8%), weight SPAD (18.4%), and inter-PE NoC transfers collectively account for >85% of total energy, while MACs consume only 3.8%. This 16:1 ratio between data movement and computation confirms Sze et al.’s hierarchy [79] and motivates dataflow-centric design exploration. Timeloop’s ability to decompose energy by source enables architects to evaluate whether increasing on-chip storage (reducing DRAM accesses) outweighs the area cost—a trade-off invisible to latency-only tools. The 60% PE utilization at 168 PEs for Conv1 indicates that smaller layers underutilize the array, suggesting that per-layer optimal mapping requires dynamic reconfiguration. The estimated latency of 5.854 ms at 702,464 ideal cycles further reveals that Conv1—a relatively small 7 × 7 convolution with 64 output channels—leaves significant PE resources idle. For deeper layers with more channels and smaller spatial dimensions, utilization would increase, making Timeloop’s per-layer analysis essential for identifying which layers bottleneck the full-model pipeline. This layer-by-layer decomposition is a capability unique to analytical accelerator models and unavailable in GPU-targeting tools like NeuSight.

Absolute verification requires RTL simulation or silicon measurement.

7.5 nn-Meter: Complete Failure

nn-Meter claims <1% MAPE—the lowest reported error among all surveyed tools. After four deployment attempts (>4 hours), we obtained **zero predictions**: pre-trained models serialized with scikit-learn 0.23.1 (2020) cannot be deserialized with current versions. Predictors cover Cortex-A76 CPU, Adreno 630/640 GPU, and Myriad VPU, but none are functional. **The tool claiming the best accuracy is the only tool that produces no output**—pickle

Table 9: Tool coverage of MLPerf-Survey-2026 benchmark suite (36 scenarios). S=Supported, P=Partial, U=Unsupported. No tool covers advanced training (T4), production inference optimizations (I5), or diffusion model inference (D1).

Category	#	Neu.	AST.	VID.	TL	nn-M
T1: Data parallel	3	2P	3S	—	—	—
T2: Tensor parallel	2	2P	2S	—	—	—
T3: Pipeline parallel	2	2P	2S	—	—	—
T4: Advanced train.	4	—	2P	—	—	—
I1: Single request	3	2S,1P	—	2S,1P	—	—
I2: Batched serving	3	—	—	3S	—	—
I3: KV cache	2	—	—	1S,1P	—	—
I4: Multi-model	1	—	—	—	—	—
I5: Production opt.	4	—	—	—	—	—
Supported	5	7	6	0	0	0
Partial	3	2	2	0	0	0
Coverage	18%	25%	21%	0%	0%	0%

serialization without version pinning created an expiration date, rendering the tool unusable within two years. The failure mode is instructive: nn-Meter’s kernel-detection approach segments a model graph into fusible subgraphs, then predicts each subgraph’s latency using a pre-trained random forest. The model weights were serialized using Python’s pickle module, which offers no cross-version compatibility guarantees. When scikit-learn’s internal representation changed (versions 0.23→1.0+), all four predictors became unloadable. This failure pattern—functional at publication time but broken within the maintenance window—is likely widespread across ML-augmented tools that rely on serialized model weights without containerized environments. Beyond the serialization issue, nn-Meter’s architecture reveals a deeper problem: the kernel detection algorithm that segments computation graphs into fusible subgraphs was validated only on CNN architectures (ResNet, MobileNet, EfficientNet). Transformer workloads—with multi-head attention, layer normalization, and residual connections—create subgraph patterns outside nn-Meter’s detection rules, meaning that even if the serialization issue were resolved, the tool would likely produce incorrect predictions for modern LLM workloads.

7.6 Benchmark Suite Coverage

Table 9 evaluates each tool against our 36-scenario LLM benchmark suite. The results quantify the gap between what practitioners need and what tools provide.

Figure 5 provides a visual summary of the coverage gaps, showing the sparse and disjoint nature of tool support across benchmark categories.

Over half of workloads have zero tool coverage. Of 36 scenarios, 20 (56%) are not addressable by any evaluated tool. The entirely uncovered scenarios include FP8 mixed-precision training (T4.1), LoRA fine-tuning (T4.2), DeepSeek MoE training (T4.5–T4.6), speculative decoding (I5.1), prefix caching (I5.2), INT4 quantized inference (I5.3), disaggregated serving (I5.4), multi-model co-location (I4.1–I4.2), and all diffusion model scenarios (D1.1–D1.3). These represent the fastest-growing deployment patterns in production

Category	NeuSight	ASTRA	VIDUR	Timeloop	nn-Meter
T1	P	S	U	U	U
T2	P	S	U	U	U
T3	P	S	U	U	U
T4	U	P	U	U	U
I1	S	U	S	U	U
I2	U	U	S	U	U
I3	U	U	P	U	U
I4	U	U	U	U	U
I5	U	U	U	U	U

S Supported **P** Partial **U** Unsupported

Figure 5: Tool×workload coverage heatmap for the 36-scenario benchmark suite. Training categories T1–T4, inference categories I1–I5, and diffusion D1. Green=supported, yellow=partial, red=unsupported. Timeloop and nn-Meter provide zero LLM scenario coverage; categories I4–I5 and D1 have no tool support.

generative-AI systems. Sequence parallelism (T4.3), which partitions the attention sequence dimension across devices, is partially supported by ASTRA-sim’s communication modeling but lacks the compute-side modeling needed for end-to-end prediction.

Tools cover disjoint slices with minimal overlap. ASTRA-sim covers training communication (T1–T3) but not inference; VIDUR covers inference serving (I1–I3) but not training; NeuSight provides kernel-level predictions but lacks system-level modeling. Only 3 scenarios (I1.1, I1.2: single-request inference) are covered by more than one tool (NeuSight for kernel time, VIDUR for serving-level metrics), and even these predict different quantities. This disjointness means that for 33 of 36 scenarios (92%), practitioners have at most one tool option—and for 20 scenarios, they have none. The practical consequence is that no single tool can answer end-to-end deployment questions like “What throughput will Llama-2-70B achieve on 32XH100 with tensor parallelism under Sarathi-Serve at QPS 8?”—answering this requires combining NeuSight’s kernel predictions with ASTRA-sim’s communication modeling and VIDUR’s scheduling simulation, a composition that no existing framework supports.

Modern techniques are the largest gap. Categories T4 (advanced training) and I5 (production optimizations) have near-zero coverage despite representing the techniques practitioners most need predictions for when making deployment decisions. MoE expert parallelism (T4.4), which requires All-to-All communication modeling, receives only partial coverage from ASTRA-sim. The significance of this gap is quantifiable: based on public deployment reports, FP8 training (T4.1) reduces GPU memory consumption by ~2× and is now the default precision for Llama-3 pre-training; LoRA fine-tuning (T4.2) accounts for the majority of production

929 fine-tuning workloads; and speculative decoding (I5.1) is deployed
 930 in production at multiple LLM serving providers. A tool ecosystem
 931 that cannot model these dominant techniques forces practitioners
 932 to rely on empirical trial-and-error for their most consequential
 933 deployment decisions.

934 **Per-scenario gap analysis.** The 20 entirely uncovered scenarios
 935 cluster into four groups. *Training-side gaps* (T4.1–T4.3): FP8 mixed-
 936 precision training changes the arithmetic intensity of every kernel,
 937 requiring tools to model reduced-precision tensor cores; LoRA fine-
 938 tuning introduces adapter layers with different compute profiles
 939 than full-rank layers; sequence parallelism partitions the sequence
 940 dimension across devices, creating communication patterns that
 941 none of the evaluated tools model. *Inference-side gaps* (I5.1–I5.4):
 942 speculative decoding requires modeling the acceptance probability
 943 and tree-structured verification, creating variable-length execution
 944 paths; prefix caching changes the KV cache access pattern from
 945 sequential to random; INT4/INT8 quantized inference alters both
 946 compute intensity and memory bandwidth utilization; disaggregated
 947 serving (separating prefill and decode to different GPU pools)
 948 introduces inter-pool network transfer that no tool simulates. *Multi-
 949 model gaps* (I4.1–I4.2): co-locating multiple models on shared GPUs
 950 creates memory and compute contention that requires fine-grained
 951 resource modeling beyond what any evaluated tool provides. *Dif-
 952 fusion model gaps* (D1.1–D1.3): iterative denoising with U-Net or
 953 transformer backbones, classifier-free guidance doubling compute,
 954 and latent-space operations create workload patterns fundamen-
 955 tally different from autoregressive LLM inference that no evaluated
 956 tool addresses.

957 **Failure mode taxonomy for uncovered scenarios.** The 20
 958 uncovered scenarios fail for three distinct reasons, each requiring
 959 different tool extensions. *Missing algorithmic primitives:* speculative
 960 decoding (I5.1) and prefix caching (I5.2) introduce algorithmic
 961 constructs—tree-structured verification and hash-indexed KV cache
 962 lookup—that lie outside the operator-level abstractions used by all
 963 five tools. Supporting these scenarios requires extending tool input
 964 specifications to accept algorithm-level parameters (e.g., draft model
 965 acceptance rate, prefix hit ratio) rather than only architecture-level
 966 parameters. *Missing hardware models:* FP8 training (T4.1) and INT4
 967 inference (I5.3) require quantized arithmetic intensity models that
 968 account for reduced-precision tensor core throughput, dequantization
 969 overhead, and mixed-precision accumulation—none of which
 970 are modeled by NeuSight’s fp16/fp32 tile decomposition or ASTRA-
 971 sim’s communication-only simulation. *Missing system-level interactions:*
 972 disaggregated serving (I5.4), multi-model co-location (I4.1–
 973 I4.2), and diffusion model pipelines (D1) create cross-component
 974 interference (network contention between prefill and decode pools,
 975 GPU memory pressure between co-located models, iterative denois-
 976 ing scheduling) that requires coupling otherwise independent tool
 977 components.

978 **Coverage concentration.** The 16 covered scenarios concen-
 979 trate in categories T1–T3 (basic parallel training) and I1–I3 (basic
 980 inference and serving). This coverage pattern reflects the tempo-
 981 ral development of tools: ASTRA-sim (2020/2023) targets pre-LLM
 982 distributed training patterns, while VIDUR (2024) targets early
 983 LLM serving before speculative decoding and disaggregated ar-
 984 chitectures became prevalent. The field’s tool development lags
 985 deployment practice by 1–2 years. This temporal lag has practical

986 consequences: by the time a tool supporting speculative decod-
 987 ing is developed and validated, practitioners will have moved to
 988 next-generation serving techniques (e.g., tree-structured specula-
 989 tive decoding with multiple draft models, or hybrid prefill-decode
 990 disaggregation), perpetuating the coverage gap. Breaking this cycle
 991 requires either dramatically faster tool development or modular
 992 tool architectures that can incorporate new techniques as plugins
 993 rather than requiring fundamental redesigns.

994 **Aggregate coverage by tool.** Combining supported and partial
 995 scenarios, ASTRA-sim provides the broadest LLM-relevant cover-
 996 age ($11/36 = 31\%$), followed by VIDUR ($9/36 = 25\%$) and NeuSight
 997 ($9/36 = 25\%$). However, ASTRA-sim’s coverage is concentrated in
 998 training (T1–T4) while VIDUR’s is concentrated in inference (I1–I3),
 999 reinforcing the complementarity finding. The union of all five tools
 1000 covers only 16 of 36 scenarios (44%), with the remaining 20 requir-
 1001 ing entirely new tool development. Notably, even the “supported”
 1002 scenarios often predict different metrics: for single-request infer-
 1003 ence (I1.1), NeuSight predicts kernel execution time while VIDUR
 1004 predicts end-to-end serving latency including scheduling delay and
 1005 KV cache allocation—two quantities separated by the composition
 1006 gap.

1007 **Coverage quality varies within “supported” scenarios.** Even
 1008 among the 16 covered scenarios, support quality is uneven. For T1.1
 1009 (data-parallel GPT-2 on $8 \times \text{A100}$), NeuSight provides only per-GPU
 1010 kernel time (partial) while ASTRA-sim provides full communication
 1011 modeling (supported)—but neither tool produces the end-to-end
 1012 iteration time that practitioners optimize. For I2.1 (batched Llama-2-
 1013 7B serving under vLLM), VIDUR provides full end-to-end prediction
 1014 including scheduling, preemption, and KV cache management—the
 1015 most complete single-tool coverage for any scenario in our suite.
 1016 This disparity illustrates that a binary supported/unsupported met-
 1017 ric, while useful for aggregate analysis, masks significant variation
 1018 in prediction completeness that affects practitioner trust and adop-
 1019 tion.

7.7 Cross-Cutting Findings

1020 Four findings emerge from combining accuracy verification with
 1021 benchmark coverage analysis:

1022 **First, self-reported accuracy is inversely correlated with
 1023 reliability.** By claimed accuracy: nn-Meter ($<1\%$) > NeuSight (2.3%)
 1024 > VIDUR ($<5\%$) > Timeloop (5–10%) > ASTRA-sim (5–15%). By
 1025 actual reliability: VIDUR/ASTRA-sim (Docker, valid output in <30
 1026 min) > Timeloop > NeuSight (accuracy overstated) > nn-Meter
 1027 (broken). The tools claiming the lowest error are the least reliable.

1028 **Second, the five tools are complementary, not competing.**
 1029 No two tools meaningfully overlap: NeuSight predicts GPU kernels;
 1030 ASTRA-sim simulates communication; VIDUR models LLM serving;
 1031 Timeloop explores accelerator design; nn-Meter targets edge. The
 1032 field needs a *unified pipeline* combining tool strengths (Section 8).

1033 **Third, the composition gap dominates end-to-end error.**
 1034 NeuSight’s kernel-level 5–9% MAPE grows to 10–28% at model
 1035 level. The 5–15% composition error—launch overhead, memory al-
 1036 location, synchronization—is *larger than kernel-level error*. Improv-
 1037 ing kernel predictors has diminishing returns until composition is
 1038 solved (Figure 7).

Fourth, 50% of modern LLM workloads lack any modeling tool. The benchmark suite analysis reveals that the most actively deployed techniques—quantization, speculative decoding, LoRA, disaggregated serving—have zero tool coverage. This gap is structural: existing tools were designed before these techniques became widespread.

Fifth, deployment robustness varies inversely with model complexity. Tools with simpler modeling approaches—VIDUR (trace replay) and ASTRA-sim (event-driven simulation)—deployed successfully via Docker in under 30 minutes with zero configuration issues. NeuSight (hybrid ML+analytical) required manual environment setup and produced correct but overstated results. nn-Meter (pure ML-augmented) failed entirely. Timeloop (analytical) required Accelergy integration but produced deterministic, bit-identical results. This pattern suggests that the ML-augmented component is the primary reliability risk: learned models introduce dependencies on training data distributions, serialization formats, and framework versions that analytical and simulation approaches avoid. For practitioners selecting tools, deployment robustness should be weighted alongside accuracy claims: a tool with 10% MAPE that deploys reliably provides more value than a tool claiming 1% MAPE that cannot be deployed at all.

Sixth, inference and training accuracy diverge systematically. Across NeuSight’s 146 configurations, inference accuracy (mean MAPE: 5.87–27.10% depending on device) is consistently better than training accuracy for NVIDIA GPUs (V100: 5.87% inf vs. 8.91% train; A100-80G: 8.63% inf vs. 7.59% train is the only exception). For AMD GPUs, the gap is larger: MI100 shows 10.80% inference vs. 15.62% training; MI210 shows 8.40% vs. 15.73%. Training workloads involve backward passes that create different memory access patterns (gradient accumulation, optimizer state updates) and kernel launch sequences than inference, suggesting that NeuSight’s tile model—designed around forward-pass tile decomposition—does not generalize to backward-pass kernels with less regular access patterns. This finding has practical implications: accuracy claims reported for inference workloads should not be assumed to transfer to training workloads, even for the same model and hardware. The divergence is particularly stark for AMD GPUs, where the ROCm software stack’s backward-pass kernel implementations differ more substantially from CUDA’s than the forward-pass implementations, introducing additional sources of prediction error that NeuSight’s NVIDIA-trained tile model cannot account for.

Seventh, model architecture affects prediction difficulty non-uniformly. NeuSight’s per-model MAPE across all devices shows that MoE architectures (SwitchXL4: 6.33–17.65% APE range across configurations) exhibit higher variance than dense models (OPT-13B: 0.38–10.53%; GPT-3-2.7B: 0.43–7.73%). The higher variance for MoE arises because expert routing creates workload-dependent computation patterns that a static tile decomposition cannot fully capture. This observation extends to future tools: MoE, sparse attention, and dynamic architectures will likely require workload-aware prediction mechanisms rather than architecture-only models.

These seven findings, when mapped against our 36-scenario benchmark suite, reveal a systematic pattern: the scenarios with the highest practitioner demand (T4, I5) coincide with the scenarios having zero or minimal tool coverage. Benchmark categories T4

Table 10: Deployment experience for each evaluated tool. Time excludes download. Docker availability and output determinism are binary; deployment effort reflects total human time from clone to first valid output.

Tool	Docker	Time	Determ.	Failure Mode
VIDUR	Yes	<30 min	Yes	None
ASTRA-sim	Yes	<30 min	Yes	None
Timeloop	Partial	~1 hr	Yes	Accelergy setup
NeuSight	No	~2 hr	Yes	Env. config
nn-Meter	No	4+ hr	N/A	Serialization

(advanced training), I5 (production optimizations), and D1 (diffusion) collectively represent 13 of 36 scenarios (36% of the suite) but account for 0 fully supported scenarios across all five tools. Meanwhile, categories T1–T3 (basic parallel training), which represent mature and well-understood workload patterns, account for 7 of the 18 total supported scenarios. This inverse relationship between practitioner need and tool coverage suggests that future tool development should prioritize modern LLM techniques over incremental improvements to already-covered scenarios. Concretely, a tool achieving even 20% MAPE on speculative decoding (I5.1) or disaggregated serving (I5.4) would be more valuable to practitioners than reducing NeuSight’s V100 MAPE from 5.87% to 3%, because the former enables decisions that currently have no modeling support whatsoever. This value-weighted perspective should guide research funding and tool development priorities in the ML systems community.

7.8 Deployment Experience and Reproducibility

Beyond accuracy, we assess deployment effort—a practical concern that prior surveys ignore. Table 10 summarizes our experience deploying each tool from scratch.

Docker availability is the strongest predictor of deployment success. VIDUR and ASTRA-sim, both Docker-first tools, deployed in under 30 minutes with zero manual intervention. Timeloop required partial manual setup for its Accelergy energy estimation plugin but produced results within one hour. NeuSight required manual Python environment configuration and model weight downloads but eventually succeeded. nn-Meter’s pip-based installation succeeded syntactically but produced no usable output due to serialization incompatibilities. This represents the worst deployment outcome: silent success at install time masking complete failure at inference time, with no diagnostic error message until the user attempts to load a predictor—a failure pattern that undermines trust in the broader ML-augmented tool ecosystem.

Extended tool evaluation. Beyond the five primary tools, we attempted deployment of five additional tools to assess the broader ecosystem’s accessibility (Table 11). MAESTRO [43] was the only additional tool that fully built and ran on our platform (macOS ARM64), producing dataflow analysis for ResNet-50 in under one minute—consistent with its CPU-only C++17 design. Paleo [62] installed via pip and produced network architecture summaries, but its simulation and profiling modes failed: cuDNN is required for convolution timing, and the TensorFlow backend requires TF 0.12 (Python 2.7 era), rendering the tool effectively unmaintained since 2018.

Table 11: Extended deployment evaluation: 5 additional tools tested on Apple M2 Ultra (macOS ARM64). Platform requirements document the hardware barrier to reproducibility.

Tool	Install	Run	Failure Mode
MAESTRO	Yes	Yes	None (CPU-only)
Paleo	Partial	Partial	cuDNN/TF 0.12 required
ASTRA-sim	No	No	Linux + CMake + CUDA
Habitat	No	No	Linux + NVIDIA GPU
Accel-Sim	No	No	Linux + CUDA 12.x

ASTRA-sim [86], Habitat [89], and Accel-Sim [38] all require Linux with NVIDIA GPUs and CUDA toolkits, making them inaccessible on our Apple Silicon test platform. These platform-unavailability results are themselves informative: they document the hardware barrier that prevents many researchers from reproducing published results, particularly those without access to NVIDIA datacenter GPUs. In total, we evaluated 10 tools: 5 with full experimental results and 5 with documented deployment outcomes including failure modes.

Determinism varies by methodology. All evaluated tools except nn-Meter (which produced no output) generated bit-identical results across three independent runs on the same platform. This determinism is notable for NeuSight, whose hybrid ML+analytical approach could in principle exhibit stochastic behavior; the determinism arises because NeuSight uses fixed pre-trained weights and analytical tile decomposition with no stochastic inference-time components. Deterministic outputs simplify regression testing and enable exact reproducibility—properties that should be standard but are not guaranteed by ML-augmented tools that use stochastic inference (e.g., dropout at test time, Monte Carlo sampling for uncertainty quantification).

7.9 Threats to Validity

External validity. Our venue-focused search may under-represent industry tools. We exclude proprietary tools from evaluation. The benchmark suite’s 36 scenarios, while representative, cannot cover every production deployment pattern; emerging workloads (e.g., retrieval-augmented generation, multi-modal models) are not yet included.

Internal validity. Our full experiments cover 5 of 25 tools, with deployment testing on 5 additional tools (10 total). Findings rest on single tool instances per methodology type—e.g., nn-Meter may be unrepresentative due to deployment failure. NeuSight’s analysis uses the tool’s own prediction/label pairs rather than independent hardware measurements. The per-device sample sizes vary (3–18 configurations), limiting statistical power for devices with few data points (e.g., P4 with only 3 configurations, A100-SXM with 3 configurations). We mitigate this by reporting both mean and worst-case APE. Our benchmark suite covers 36 scenarios, but the distribution is not uniform: training scenarios (15) and inference scenarios (18) are complemented by diffusion scenarios (3), with multi-model scenarios (14) and diffusion scenarios (D1) having the fewest entries per category. A more balanced suite might weight scenarios by practitioner frequency of use, but such weighting data is not publicly available. Despite these limitations, our suite provides the first

standardized coverage metric for ML performance tools, enabling future evaluations to quantitatively compare tool ecosystems.

Construct validity. Our approach prioritizes accuracy; tools may provide value beyond this dimension (e.g., Timeloop’s energy breakdown for design insight, ASTRA-sim’s what-if analysis for topology exploration). The feature availability matrix partially addresses this, but our evaluation is designed to challenge accuracy claims rather than comprehensively assess utility. Additionally, our coverage criterion (supported/partial/unsupported) does not capture the quality of partial support—ASTRA-sim’s partial coverage of MoE training (T4.4), for example, provides All-to-All communication modeling but misses expert load balancing effects. A finer-grained coverage metric—e.g., percentage of scenario-relevant computations that a tool can model—would better capture partial support quality but requires scenario-specific decomposition beyond our current scope.

Temporal validity. Our evaluation reflects tool state as of January 2026. Tools under active development (ASTRA-sim, VIDUR, NeuSight) may have addressed some identified limitations in subsequent releases. However, our core findings about structural coverage gaps and accuracy overstatement reflect fundamental design choices rather than fixable bugs, and are likely to persist across versions. We encourage future evaluations to adopt this third-party evaluation methodology and benchmark suite to enable longitudinal tracking of tool accuracy. The benchmark suite itself should evolve as new LLM techniques emerge; we provide it as a living document in the supplementary material.

Benchmark suite validity. The MLPerf-Survey-2026 benchmark suite was designed around the LLM and generative-AI workload landscape as of early 2026. Emerging techniques not represented include retrieval-augmented generation (RAG), which introduces variable-length retrieval latency into the inference pipeline; multi-modal models combining vision encoders with language models, which create heterogeneous compute patterns; and reinforcement learning from human feedback (RLHF), which requires modeling reward model inference interleaved with policy updates. We designed the suite to be extensible: each scenario is specified by a tuple of (model architecture, hardware configuration, parallelism strategy, target metric), allowing new scenarios to be added as techniques mature without restructuring the evaluation framework. Future versions should expand beyond 40 scenarios to maintain coverage as the generative-AI deployment landscape diversifies.

8 Toward a Unified Simulation Pipeline

No single tool spans kernel execution through serving SLAs. Figure 6 shows five layers where 5–9% kernel MAPE grows to 10–28% at model level, driven by (i) interface heterogeneity, (ii) calibration mismatch between steady-state models and transient-dominated kernels, and (iii) feedback loops in serving schedulers.

9 Open Challenges and Future Directions

(1) Composition gap: Kernel errors of 2–3% yield 5–12% model-level error (Figure 7) with no validated pipeline. **(2) Frontier workloads:** MoE, diffusion [40], and dynamic inference lack validated tools; scaling laws [14, 22, 27, 37] predict loss but not latency (Figure 8). **(3) Hardware transfer:** Cross-family transfer (GPU→TPU→PIM [26,

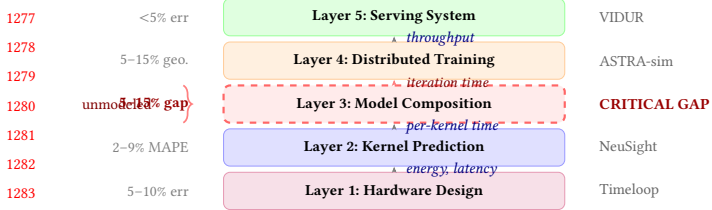


Figure 6: Unified five-layer pipeline. Layer 3 (dashed) is the critical unmodeled gap.

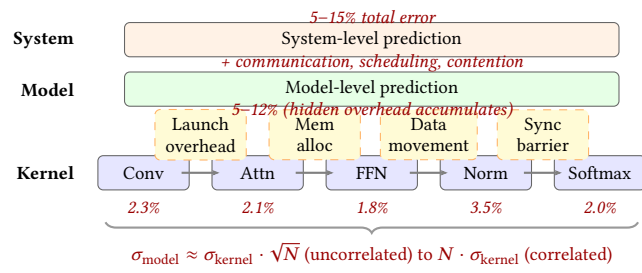


Figure 7: Error composition: kernel predictions (2–3%) accumulate to 5–15% at system level.

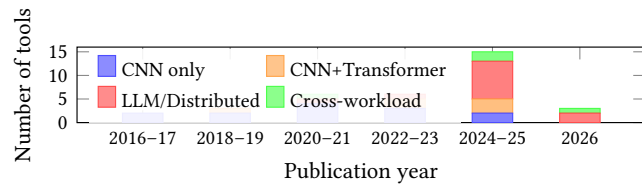


Figure 8: Workload coverage by publication period. MoE and diffusion models remain uncharacterized.

31, 46, 59]) and congestion modeling [49, 86] remain unsolved. **(4) Standardized evaluation:** No MLPerf [54, 68, 69] equivalent exists for simulators; portable formats [75] and continuous validation are needed; concurrent surveys [77] similarly identify this gap. **(5) Reproducibility:** nn-Meter failed from dependency rot; containerization and CI testing are needed. **(6) Software stack evolution:** Rapidly evolving optimizations such as FlashAttention [16] invalidate performance models trained on prior kernel implementations.

10 Conclusion

We survey 25 ML performance tools and evaluate ten against a 36-scenario benchmark, finding self-reported accuracy unreliable (NeuSight: 2.3% claimed vs. 5.87–27.10%; nn-Meter: no output). The 5–15% composition gap dominates total error; closing it requires validated composition models and community CI.

References

- [1] Martin Abadi, Paul Barham, Jianmin Chen, Zhifeng Chen, Andy Davis, Jeffrey Dean, Matthieu Devin, Sanjay Ghemawat, Geoffrey Irving, Michael Isard, et al. 2016. TensorFlow: A System for Large-Scale Machine Learning. In *Proceedings of the 12th USENIX Symposium on Operating Systems Design and Implementation (OSDI)*. 265–283.
- [2] Amey Agrawal, Nitin Kedia, Ashish Panwar, Jayashree Mohan, Nipun Kwatra, Bhargav S. Gulavani, Alexey Tumanov, and Ramachandran Ramachandran. 2024. Taming Throughput-Latency Tradeoff in LLM Inference with Sarathi-Serve. In *Proceedings of the 18th USENIX Symposium on Operating Systems Design and Implementation (OSDI)*. 117–134.
- [3] Amey Agrawal, Ashish Panwar, Jayashree Mohan, Nipun Kwatra, Bhargav S. Gulavani, and Ramachandran Ramachandran. 2024. VIDUR: A Large-Scale Simulation Framework for LLM Inference. In *Proceedings of Machine Learning and Systems (MLSys)*. 1–15.
- [4] Ali Bakhoda, George L. Yuan, Wilson W. L. Fung, Henry Wong, and Tor M. Aamodt. 2009. Analyzing CUDA Workloads Using a Detailed GPU Simulator. In *Proceedings of the IEEE International Symposium on Performance Analysis of Systems and Software (ISPASS)*. 163–174. <https://doi.org/10.1109/ISPASS.2009.4919648>
- [5] Abhimanyu Rajeshkumar Bambhaniya et al. 2025. HERMES: Understanding and Optimizing Multi-Stage AI Inference Pipelines. *arXiv preprint arXiv:2504.09775* (2025). Heterogeneous multi-stage LLM inference simulator with analytical modeling.
- [6] Nathan Binkert, Bradford Beckmann, Gabriel Black, Steven K. Reinhardt, Ali Saidi, Arkaprava Basu, Joel Hestness, Derek R. Hower, Tushar Krishna, Somayeh Sardashti, Rathijit Sen, Korey Sewell, Muhammad Shoib, Nilay Vaish, Mark D. Hill, and David A. Wood. 2011. The gem5 Simulator. *ACM SIGARCH Computer Architecture News* 39, 2 (2011), 1–7. <https://doi.org/10.1145/2024716.2024718>
- [7] Shirley Browne, Jack Dongarra, Nathan Garner, George Ho, and Philip Mucci. 2000. A Portable Programming Interface for Performance Evaluation on Modern Processors. *International Journal of High Performance Computing Applications* 14, 3 (2000), 189–204. <https://doi.org/10.1177/109434200001400303> PAPI: portable API for hardware performance counters, foundational tool for performance analysis.
- [8] Kai Cai, Wei Miao, Junyu Zhu, Jiaxu Chen, Hao Shan, Huanyu Li, and Chi Zhang. 2024. Echo: Simulating Distributed Training At Scale. *arXiv preprint arXiv:2412.12487* (2024).
- [9] Tianle Cai, Yuhong Li, Zhengyang Geng, Hongwu Peng, Jason D. Lee, Deming Chen, and Tri Dao. 2024. MEDUSA: Simple LLM Inference Acceleration Framework with Multiple Decoding Heads. In *Proceedings of the 41st International Conference on Machine Learning (ICML)*. 1–15.
- [10] Zheng Cao et al. 2025. AMALI: An Analytical Model for Accurately Modeling LLM Inference on Modern GPUs. In *Proceedings of the 52nd Annual International Symposium on Computer Architecture (ISCA)*. 1–14. <https://doi.org/10.1145/3695053.3731064> Reduces GPU LLM inference MAPE from 127.56% to 23.59% vs GCoM baseline.
- [11] Tianshi Chen, Zidong Du, Ninghui Sun, Jia Wang, Chengyong Wu, Yunji Chen, and Olivier Temam. 2014. DianNao: A Small-Footprint High-Throughput Accelerator for Ubiquitous Machine-Learning. In *Proceedings of the 19th International Conference on Architectural Support for Programming Languages and Operating Systems (ASPLOS)*. 269–284. <https://doi.org/10.1145/2541940.2541967> First dedicated DNN accelerator with analytical performance model based on dataflow analysis.
- [12] Tianqi Chen, Thierry Moreau, Ziheng Jiang, Lianmin Zheng, Eddie Yan, Meghan Cowan, Haichen Shen, Leyuan Wang, Yuwei Hu, Luis Ceze, Carlos Guestrin, and Arvind Krishnamurthy. 2018. TVM: An Automated End-to-End Optimizing Compiler for Deep Learning. In *Proceedings of the 13th USENIX Symposium on Operating Systems Design and Implementation (OSDI)*. 578–594.
- [13] Yu-Hsin Chen, Joel Emer, and Vivienne Sze. 2016. Eyeriss: A Spatial Architecture for Energy-Efficient Dataflow for Convolutional Neural Networks. In *Proceedings of the 43rd International Symposium on Computer Architecture (ISCA)*. 367–379. <https://doi.org/10.1109/ISCA.2016.40>
- [14] Leshem Choshen, Yang Zhang, and Jacob Andreas. 2025. A Hitchhiker’s Guide to Scaling Law Estimation. In *Proceedings of the 42nd International Conference on Machine Learning (ICML)*. 1–25. Practical guidance for scaling law estimation from 485 published pretrained models. IBM/MIT..
- [15] Weiwei Chu, Xinfeng Xie, Jiecao Yu, Jie Wang, Pavani Balaji, Ching-Hsiang Chu, Jongsoo Park, et al. 2025. Scaling Llama 3 Training with Efficient Parallelism Strategies. In *Proceedings of the 52nd Annual International Symposium on Computer Architecture (ISCA)*. 1–15. 4D parallelism for Llama 3 405B on 16K H100 GPUs. Achieves 400 TFLOPS/GPU. Meta..
- [16] Tri Dao, Dan Fu, Stefano Ermon, Atri Rudra, and Christopher Ré. 2022. FlashAttention: Fast and Memory-Efficient Exact Attention with IO-Awareness. In *Advances in Neural Information Processing Systems (NeurIPS)*, Vol. 35. 16344–16359.
- [17] Lukasz Dudziak, Thomas Chau, Mohamed S. Abdelfattah, Roysen Lee, Hyeji Kim, and Nicholas D. Lane. 2024. Latency Predictors for Neural Architecture Search. In *Proceedings of Machine Learning and Systems (MLSys)*. 1–14.
- [18] Yang Feng, Zhehao Li, Jiacheng Yang, and Yunxin Liu. 2024. LitePred: Transferable and Scalable Latency Prediction for Hardware-Aware Neural Architecture Search. In *Proceedings of the 21st USENIX Symposium on Networked Systems Design and Implementation (NSDI)*. 1–18.

1335
1336
1337
1338
1339
1340
1341
1342
1343
1344
1345
1346
1347
1348
1349
1350
1351
1352
1353
1354
1355
1356
1357
1358
1359
1360
1361
1362
1363
1364
1365
1366
1367
1368
1369
1370
1371
1372
1373
1374
1375
1376
1377
1378
1379
1380
1381
1382
1383
1384
1385
1386
1387
1388
1389
1390
1391
1392

- 1393 [19] Paraskevas Gavrilidis et al. 2025. LIFE: Forecasting LLM Inference Performance
1394 via Hardware-Agnostic Analytical Modeling. *arXiv preprint arXiv:2508.00904*
1395 (2025). Hardware-agnostic analytical model for LLM inference performance
1396 forecasting.
- 1397 [20] Siddharth Ghosh et al. 2025. Frontier: Simulating the Next Generation of LLM
1398 Inference Systems. *arXiv preprint arXiv:2508.03148* (2025). Stage-centric simulator
1399 for MoE and disaggregated LLM inference, models expert parallelism and cross-
1400 cluster routing.
- 1401 [21] Alicia Golden et al. 2025. PRISM: Probabilistic Runtime Insights and Scalable
1402 Performance Modeling for Large-Scale Distributed Training. *arXiv preprint arXiv:2510.15590*
1403 (2025). Probabilistic performance modeling for distributed
1404 training at 10K+ GPU scale. Meta..
- 1405 [22] Alexander Hagele, Elie Bakouch, Atli Kosson, Loubna Ben Allal, Leandro
1406 Von Werra, and Martin Jaggi. 2024. Scaling Laws and Compute-Optimal Training
1407 Beyond Fixed Training Durations. In *Advances in Neural Information Processing
1408 Systems (NeurIPS)*, Vol. 37. Spotlight. Practical scaling laws with constant LR +
1409 cooldowns for reliable training compute prediction..
- 1410 [23] Ameer Haj-Ali et al. 2025. Omniwise: Predicting GPU Kernels Performance with
1411 LLMs. *arXiv preprint arXiv:2506.20886* (2025). First LLM-based GPU kernel
1412 performance prediction, 90% within 10% error on AMD MI250/MI300X.
- 1413 [24] Yanbin Hao et al. 2025. POD-Attention: Unlocking Full Prefill-Decode Overlap
1414 for Faster LLM Inference. In *Proceedings of the 30th ACM International Conference
1415 on Architectural Support for Programming Languages and Operating Systems (ASPLOS)*.
1416 1–15. Full overlap between prefill and decode phases for LLM inference.
- 1417 [25] John L. Hennessy and David A. Patterson. 2019. A New Golden Age for Computer
1418 Architecture. *Commun. ACM* 62, 2 (2019), 48–60. <https://doi.org/10.1145/3282307>
1419 Turing Award Lecture: domain-specific architectures and the end of Dennard
1420 scaling.
- 1421 [26] Guseul Heo, Sangyeop Lee, Jaehong Cho, Hyunmin Choi, Sanghyeon Lee,
1422 Hyungkyu Ham, Gwangsun Kim, Divya Mahajan, and Jongse Park. 2024. NeuPIMs:
1423 NPU-PIM Heterogeneous Acceleration for Batched LLM Inferencing. In
1424 *Proceedings of the 29th ACM International Conference on Architectural Support
1425 for Programming Languages and Operating Systems (ASPLOS)*. 1–17. NPU-
1426 PIM heterogeneous architecture for LLM inference with performance modeling.
KAIST/Georgia Tech..
- 1427 [27] Jordan Hoffmann, Sebastian Borgeaud, Arthur Mensch, Elena Buchatskaya,
1428 Trevor Cai, Eliza Rutherford, Diego de Las Casas, Lisa Anne Hendricks, Johannes
1429 Welbl, Aidan Clark, et al. 2022. Training Compute-Optimal Large Language
1430 Models. *arXiv preprint arXiv:2203.15556* (2022). Chinchilla scaling laws: compute-
1431 optimal training requires scaling data proportionally to model size.
- 1432 [28] Samuel Hsia, Kartik Chandra, and Kunle Olukotun. 2024. MAD Max Beyond
1433 Single-Node: Enabling Large Machine Learning Model Acceleration on Dis-
1434 tributed Systems. In *Proceedings of the 51st Annual International Symposium on
1435 Computer Architecture (ISCA)*. 753–766. <https://doi.org/10.1109/ISCA59077.2024.00064>
- 1436 [29] Yanping Huang, Youlong Cheng, Ankur Bapna, Orhan Firat, Dehao Chen, Mia Xu
1437 Chen, Hyoukjoong Lee, Jiquan Ngiam, Quoc V. Le, Yonghui Wu, and Zhifeng
1438 Chen. 2019. GPipe: Efficient Training of Giant Neural Networks using Pipeline
1439 Parallelism. In *Advances in Neural Information Processing Systems (NeurIPS)*,
1440 Vol. 32. 103–112.
- 1441 [30] Rodrigo Huerta, Mojtaba Abaei Shoshtary, Jose-Lorenzo Cruz, and Antonio
1442 Gonzalez. 2025. Dissecting and Modeling the Architecture of Modern GPU Cores.
In *Proceedings of the 58th IEEE/ACM International Symposium on Microarchitecture
1443 (MICRO)*. 369–384. Reverse-engineers modern NVIDIA GPU cores, improves
1444 Accel-Sim to 13.98% MAPE. UPC Barcelona..
- 1445 [31] Bongjoon Hyun, Taehun Kim, Dongjae Lee, and Minsoo Rhu. 2024. Pathfinding
1446 Future PIM Architectures by Demystifying a Commercial PIM Technology.
In *Proceedings of the IEEE International Symposium on High Performance
1447 Computer Architecture (HPCA)*. 1–15. uPIMulator: cycle-accurate PIM simulation
1448 framework for UPMEM. KAIST..
- 1449 [32] Ryota Imai, Kentaro Harada, Ryo Sato, and Toshio Nakaike. 2024. Roofline-
1450 Driven Machine Learning for Large Language Model Performance Prediction.
NeurIPS Workshop on Machine Learning for Systems (2024).
- 1451 [33] Anand Jayaraman, Wei-Lin Hu, Gauri Zhao, and Gennady Pekhimenko. 2023.
Sia: Heterogeneity-aware, Goodput-optimized ML-Cluster Scheduling. In
1452 *Proceedings of the 29th Symposium on Operating Systems Principles (SOSP)*. 642–657.
<https://doi.org/10.1145/3600006.3613175> Extends goodput optimization to het-
1453 erogeneous GPU clusters for training workloads.
- 1454 [34] Norman P. Jouppi, Doe Hyun Yoon, George Kurian, Sheng Li, Nishant Patil,
1455 James Laudon, Cliff Young, and David Patterson. 2023. TPU v4: An Optically
1456 Reconfigurable Supercomputer for Machine Learning with Hardware Support for
1457 Embeddings. *Proceedings of the 50th Annual International Symposium on Computer
1458 Architecture (ISCA)* (2023), 1–14. <https://doi.org/10.1145/3579371.3589350> 4096-
1459 chip pods with 3D optical interconnect; up to 1.7x/2.1x faster than TPU v3.
- 1460 [35] Norman P. Jouppi, Cliff Young, Nishant Patil, David Patterson, Gaurav Agrawal,
1461 Raminder Bajwa, Sarah Bates, Suresh Bhatia, Nan Boden, Al Borber, et al. 2017.
In-Datacenter Performance Analysis of a Tensor Processing Unit. In *Proceedings
1462 of the 44th Annual International Symposium on Computer Architecture (ISCA)*.
- 1463 [36] Jared Kaplan, Sam McCandlish, Tom Henighan, Tom B. Brown, Benjamin Chess,
1464 Rewon Child, Scott Gray, Alec Radford, Jeffrey Wu, and Dario Amodei. 2020.
Scaling Laws for Neural Language Models. *arXiv preprint arXiv:2001.08361*
1465 (2020). Original neural scaling laws: power-law relationships between model
1466 size, dataset size, compute, and loss.
- 1467 [38] Mahmoud Khairy, Zhesheng Shen, Tor M. Aamodt, and Timothy G. Rogers. 2020.
Accel-Sim: An Extensible Simulation Framework for Validated GPU Modeling. In
1468 *Proceedings of the 47th International Symposium on Computer Architecture (ISCA)*.
473–486. <https://doi.org/10.1109/ISCA45697.2020.00047>
- 1469 [39] Jungho Kim et al. 2025. PyTorchSim: A Comprehensive, Fast, and Accurate
1470 NPU Simulation Framework. In *Proceedings of the 58th IEEE/ACM International
1471 Symposium on Microarchitecture (MICRO)*. 1–14. <https://doi.org/10.1145/3725843.3756045> PyTorch 2-integrated NPU simulator with custom RISC-V ISA and
1472 Tile-Level Simulation.
- 1473 [40] Jiin Kim, Byeongjun Shin, Jinha Chung, and Minsoo Rhu. 2026. The Cost of
1474 Dynamic Reasoning: Demystifying AI Agents and Test-Time Scaling from an AI
1475 Infrastructure Perspective. In *Proceedings of the IEEE International Symposium
1476 on High Performance Computer Architecture (HPCA)*. 1–14. HPCA 2026 (Jan 31–
Feb 4, 2026, Las Vegas). First comprehensive system-level analysis of AI agents;
1477 quantifies resource usage, latency, and datacenter power consumption.
- 1478 [41] Yoongi Kim, Weikun Yang, and Onur Mutlu. 2016. Ramulator: A Fast and
1479 Extensible DRAM Simulator. *IEEE Computer Architecture Letters* 15, 1 (2016), 45–
1480 49. <https://doi.org/10.1109/LCA.2015.2414456> Fast extensible DRAM simulator
1481 supporting DDRx, LPDDRx, GDDRx, WIOx, HBx standards.
- 1482 [42] Srivatsan Krishnan, Amir Yazdanbakhsh, Shvetank Prakash, Norman P.
1483 Jouppi, Jignesh Parmar, Hyoukjun Kim, James Laudon, and Chandrakant
1484 Narayanaswami. 2023. ArchGym: An Open-Source Gymnasium for Machine
1485 Learning Assisted Architecture Design. In *Proceedings of the 50th International
1486 Symposium on Computer Architecture (ISCA)*. 1–16. <https://doi.org/10.1145/3579371.3589049>
- 1487 [43] Hyoukjun Kwon, Prasanth Chatarasi, Michael Sarber, Michael Pellauer, Angshuman
1488 Parashar, and Tushar Krishna. 2019. MAESTRO: A Data-Centric Approach
1489 to Understand Reuse, Performance, and Hardware Cost of DNN Mappings. In
1490 *Proceedings of the 52nd IEEE/ACM International Symposium on Microarchitecture
1491 (MICRO)*. 1–14. <https://doi.org/10.1145/3352460.3358292>
- 1492 [44] Woosuk Kwon, Zhuohan Li, Siyuan Zhuang, Ying Sheng, Liannmin Zheng,
1493 Cody Hao Yu, Joseph E. Gonzalez, Hao Zhang, and Ion Stoica. 2023. Efficient
1494 Memory Management for Large Language Model Serving with PagedAttention.
In *Proceedings of the 29th Symposium on Operating Systems Principles (SOSP)*.
611–626. <https://doi.org/10.1145/3600006.3613165>
- 1495 [45] Chris Lattner, Mehdi Amini, Uday Bondhugula, Albert Cohen, Andy Davis,
1496 Jacques Pienaar, River Riddle, Tatiana Shpeisman, Nicolas Vasilache, and Oleksandr
1497 Zinenko. 2021. MLIR: Scaling Compiler Infrastructure for Domain Specific
1498 Computation. In *Proceedings of the IEEE/ACM International Symposium on Code
1499 Generation and Optimization (CGO)*. 2–14. <https://doi.org/10.1109/CGO51591.2021.9370308> Multi-level IR infrastructure enabling cost model composition
1500 across abstraction levels.
- 1501 [46] Hyojung Lee, Daehyeon Baek, Jimyoung Son, Jieun Choi, Kihyo Moon, and
1502 Minsung Jang. 2025. PAISE: PIM-Accelerated Inference Scheduling Engine for
1503 Transformer-based LLM. In *Proceedings of the IEEE International Symposium
1504 on High Performance Computer Architecture (HPCA)*. 1–14. PIM-based LLM
1505 inference scheduling. 48.3% speedup, 11.5% power reduction. Samsung..
- 1506 [47] Hayeon Lee, Sewooong Lee, Song Chong, and Sung Ju Hwang. 2021. HELP:
1507 Hardware-Adaptive Efficient Latency Prediction for NAS via Meta-Learning.
In *Advances in Neural Information Processing Systems (NeurIPS)*, Vol. 34. 27016–
1508 27028.
- 1509 [48] Seunghyun Lee, Amar Phanishayee, and Divya Mahajan. 2025. NeuSight: GPU
1510 Performance Forecasting via Tile-Based Execution Analysis. In *Proceedings of
1511 the 30th ACM International Conference on Architectural Support for Programming
1512 Languages and Operating Systems (ASPLOS)*. 1–15.
- 1513 [49] Jianbo Li et al. 2025. TrioSim: A Lightweight Simulator for Large-Scale DNN
1514 Workloads on Multi-GPU Systems. In *Proceedings of the 52nd Annual International
1515 Symposium on Computer Architecture (ISCA)*. 1–13. Multi-GPU DNN simulation
1516 with lightweight approach for distributed training analysis.
- 1517 [50] Shang Li, Zhiyuan Yang, Dhiraj Reddy, Ankur Srivastava, and Bruce Jacob. 2020.
DRAMsim3: A Cycle-Accurate, Thermal-Capable DRAM Simulator. *IEEE Computer
1518 Architecture Letters* 19, 2 (2020), 106–109. <https://doi.org/10.1109/LCA.2020.2973991> Modernized DRAM simulator with thermal modeling and HMC
1519 support.
- 1520 [51] Ying Li, Yifan Sun, and Adwait Jogi. 2023. Path Forward Beyond Simulators: Fast
1521 and Accurate GPU Execution Time Prediction for DNN Workloads. In *Proceedings
1522 of the 56th Annual International Symposium on Computer Architecture (ISCA)*.

- of the 56th Annual IEEE/ACM International Symposium on Microarchitecture (MICRO). 1–14. <https://doi.org/10.1145/3613424.3614277> Linear-regression-based DNN execution time predictor achieving 7% error for new DNN prediction and 15.2% for new GPU prediction.

[52] Wenxuan Liang et al. 2025. Lumos: Efficient Performance Modeling and Estimation for Large-scale LLM Training. In *Proceedings of Machine Learning and Systems (MLSys)*. 1–16. Trace-driven performance modeling achieving 3.3% error on H100 GPUs for LLM training.

[53] Haocong Luo, Yahya Can Tugrul, F. Nisa Bostancı, Ataberk Olgun, A. Giray Yaglikcı, and Onur Mutlu. 2023. Ramulator 2.0: A Modern, Modular, and Extensible DRAM Simulator. *IEEE Computer Architecture Letters* 22, 2 (2023), 129–132. <https://doi.org/10.1109/LCA.2023.3333759> Modular DRAM simulator with DDR5, LPDDR5, HBMs, GDDR6 support and RowHammer mitigation modeling.

[54] Peter Mattson, Christine Cheng, Cody Coleman, Greg Diamos, Paulius Micikevicius, David Patterson, Hanlin Tang, Gu-Yeon Wei, Peter Bailis, Victor Bitdorf, et al. 2020. ML-Perf Training Benchmark. In *Proceedings of Machine Learning and Systems (MLSys)*. 336–349. Standard ML training benchmark suite covering image classification, object detection, NLP, recommendation, reinforcement learning.

[55] Azaz-Ur-Rehman Nasir, Samroz Ahmad Shoaib, Muhammad Abdullah Hanif, and Muhammad Shafique. 2025. ESM: A Framework for Building Effective Surrogate Models for Hardware-Aware Neural Architecture Search. In *Proceedings of the 62nd ACM/IEEE Design Automation Conference (DAC)*. 1–6. 97.6% accuracy surrogate model framework for HW-aware NAS.

[56] Amir Nasr-Esfahany et al. 2025. Concorde: Fast and Accurate CPU Performance Modeling with Compositional Analytical-ML Fusion. In *Proceedings of the 52nd Annual International Symposium on Computer Architecture (ISCA)*. 1–15. Hybrid analytical-ML approach achieving 2% CPI error at 5 orders of magnitude faster than gem5.

[57] NVIDIA Corporation. 2019. Nsight Compute: Interactive Kernel Profiler. <https://developer.nvidia.com/nsight-compute>. Industry-standard GPU kernel profiling tool with roofline analysis.

[58] Angshuman Parashar, Priyanka Raina, Yakun Sophia Shao, Yu-Hsin Chen, Victor A. Ying, Anurag Muber, Rangharajan Venkatesan, Brucek Khailany, Stephen W. Keckler, and Joel Emer. 2019. Timeloop: A Systematic Approach to DNN Accelerator Evaluation. In *Proceedings of the IEEE International Symposium on Performance Analysis of Systems and Software (ISPASS)*. 304–315. <https://doi.org/10.1109/ISPASS.2019.00042>

[59] Jaehyun Park, Jaewon Choi, Kwanhee Kyung, Michael Jaemin Kim, Yongsuk Kwon, Nam Sung Kim, and Jung Ho Ahn. 2024. AttAcc! Unleashing the Power of PIM for Batched Transformer-based Generative Model Inference. In *Proceedings of the 29th ACM International Conference on Architectural Support for Programming Languages and Operating Systems (ASPLOS)*. 1–16. PIM-based accelerator for batched transformer attention. Seoul National University/UIUC..

[60] Adam Paszke, Sam Gross, Francisco Massa, Adam Lerer, James Bradbury, Gregory Chanan, Trevor Killeen, Zeming Lin, Natalia Gimelshein, Luca Antiga, et al. 2019. PyTorch: An Imperative Style, High-Performance Deep Learning Library. In *Advances in Neural Information Processing Systems (NeurIPS)*, Vol. 32. 8024–8035.

[61] Pratyush Patel, Esha Choukse, Chaojie Zhang, Aakanksha Shah, Íñigo Goiri, Saeed Maleki, and Ricardo Bianchini. 2024. Splitwise: Efficient Generative LLM Inference Using Phase Splitting. In *Proceedings of the 51st Annual International Symposium on Computer Architecture (ISCA)*. 118–132. <https://doi.org/10.1109/ISCA59077.2024.00019> Best Paper Award.

[62] Hang Qi, Evan R. Sparks, and Ameet Talwalkar. 2017. Paleo: A Performance Model for Deep Neural Networks. In *Proceedings of the 5th International Conference on Learning Representations (ICLR)*. <https://openreview.net/forum?id=SyVJ85lg>

[63] Aurick Qiao, Sang Keun Agrawal, Anand Jayaraman, Moustafa Mittal, Amar Altaf, Michael Cho, and Gennady Pekhimenko. 2021. Pollux: Co-adaptive Cluster Scheduling for Goodput-Optimized Deep Learning. In *Proceedings of the 15th USENIX Symposium on Operating Systems Design and Implementation (OSDI)*. 1–18. Goodput estimation for co-optimizing resource allocation and training hyperparameters.

[64] Jonathan Ragan-Kelley, Connally Barnes, Andrew Adams, Sylvain Paris, Frédo Durand, and Saman Amarasinghe. 2013. Halide: A Language and Compiler for Optimizing Parallelism, Locality, and Recomputation in Image Processing Pipelines. In *Proceedings of the 34th ACM SIGPLAN Conference on Programming Language Design and Implementation (PLDI)*. 519–530. <https://doi.org/10.1145/2491956.2462176> Pioneered separation of algorithm and schedule with learned cost models for autoscheduling.

[65] Samyam Rajbhandari, Jeff Rasley, Olatunji Rber, and Yuxiong He. 2020. ZeRO: Memory Optimizations Toward Training Trillion Parameter Models. In *Proceedings of the International Conference on High Performance Computing, Networking, Storage and Analysis (SC)*. 1–16. <https://doi.org/10.1109/SC41405.2020.00024> DeepSpeed ZeRO optimizer partitioning for memory-efficient distributed training.

[66] Mehdi Rakhshanfar and Aliakbar Zarandi. 2021. A Survey on Machine Learning-based Design Space Exploration for Processor Architectures. *Journal of Systems Architecture* 121 (2021), 102339. <https://doi.org/10.1016/j.jssarc.2021.102339>

[67] Saeed Rashidi, Srinivas Srikanvas, Kazeem Hamedani, and Tushar Krishna. 2020. ASTRA-SIM: Enabling SW/HW Co-Design Exploration for Distributed DL Training Platforms. In *Proceedings of the IEEE International Symposium on Performance Analysis of Systems and Software (ISPASS)*. 81–92. <https://doi.org/10.1109/ISPASS48437.2020.00018>

[68] Vijay Janapa Reddi et al. 2025. MLPerf Power: Benchmarking the Energy Efficiency of Machine Learning Inference. In *Proceedings of the IEEE International Symposium on High Performance Computer Architecture (HPCA)*. 1–14. Energy efficiency benchmarking for ML inference workloads.

[69] Vijay Janapa Reddi, Christine Cheng, David Kanter, Peter Mattson, Guenther Schmuelling, Carole-Jean Wu, Brian Anderson, Maxim Bresekhev, Mark Duber, et al. 2020. MLPerf Inference Benchmark. In *Proceedings of the 47th International Symposium on Computer Architecture (ISCA)*. 446–459. <https://doi.org/10.1109/ISCA45697.2020.00045> Standard ML inference benchmark suite with server and offline scenarios.

[70] George F. Riley and Thomas R. Henderson. 2010. The ns-3 Network Simulator. *Modeling and Tools for Network Simulation* (2010), 15–34. https://doi.org/10.1007/978-3-642-12331-3_2

[71] Arun F. Rodrigues, K. Scott Hemmert, Brian W. Barrett, Chad Kersey, Ron Oldfield, Marlo Weston, R. Risen, Jeanine Cook, Paul Rosenfeld, Elliott Cooper-Balis, and Bruce Jacob. 2012. The Structural Simulation Toolkit. In *ACM SIGMETRICS Performance Evaluation Review*, Vol. 38. 37–42. <https://doi.org/10.1145/1964218.1964225> Modular framework for system-level simulation, widely used for HPC and interconnect modeling.

[72] Ananda Samajdar, Yuhao Zhu, Paul Whatmough, Matthew Mattina, and Tushar Krishna. 2019. A Systematic Methodology for Characterizing Scalability of DNN Accelerators using SCALE-Sim. In *Proceedings of the IEEE International Symposium on Performance Analysis of Systems and Software (ISPASS)*. 58–68. <https://doi.org/10.1109/ISPASS.2019.00016> Cycle-accurate systolic array simulator for DNN accelerator DSE.

[73] Zhuomin Shen, Jaeho Kim, et al. 2025. AQUA: Network-Accelerated Memory Offloading for LLMs in Scale-Up GPU Domains. In *Proceedings of the 30th ACM International Conference on Architectural Support for Programming Languages and Operating Systems (ASPLOS)*. 1–16. <https://doi.org/10.1145/3676641.3715983> Improves LLM inference responsiveness by 20x through network-accelerated memory offloading.

[74] Mohammad Shoeybi, Mostafa Patwary, Raul Puri, Patrick LeGresley, Jared Casper, and Bryan Catanzaro. 2020. Megatron-LM: Training Multi-Billion Parameter Language Models Using Model Parallelism. In *arXiv preprint arXiv:1909.08053*. Intra-layer tensor parallelism for large language model training.

[75] Srinivas Sridharan, Taekyung Heo, Jinwoo Choi, Garyfallia Yu, Saeed Rashidi, William Won, Zhaodong Meng, and Tushar Krishna. 2023. Chakra: Advancing Performance Benchmarking and Co-design using Standardized Execution Traces. *arXiv preprint arXiv:2305.14516* (2023).

[76] Foteini Strati, Zhendong Zhang, George Manos, Ixeia Sanchez Periz, Qinghao Hu, Tiancheng Chen, Berk Buzcu, Song Han, Pamela Delgado, and Ana Klimovic. 2025. Sailor: Automating Distributed Training over Dynamic, Heterogeneous, and Geo-distributed Clusters. In *Proceedings of the 30th ACM Symposium on Operating Systems Principles (SOSP)*. 1–18. Automated distributed training with runtime/memory simulation over heterogeneous resources. ETH Zurich/MIT..

[77] Jonas Svedas, Hannah Watson, Nathan Laubeuf, Diksha Moolchandani, Abubakr Nada, Arjun Singh, Dwaipayan Biswas, James Myers, and Debjyoti Bhattacharjee. 2025. A Survey of End-to-End Modeling for Distributed DNN Training: Workloads, Simulators, and TCO. *arXiv preprint arXiv:2506.09275* (2025). Comprehensive survey of distributed DNN training simulators covering workload representation, simulation infrastructure, and TCO/carbon modeling.

[78] Ondrej Sykora, Alexis Rucker, Charith Mendis, Rajkishore Barik, Phitchaya Mangpo Phothilimthana, and Saman Amarasinghe. 2022. GRANITE: A Graph Neural Network Model for Basic Block Throughput Estimation. In *Proceedings of the IEEE International Symposium on Workload Characterization (IISWC)*. 1–13. <https://doi.org/10.1109/IISWC55918.2022.00014>

[79] Vivienne Sze, Yu-Hsin Chen, Tien-Ju Yang, and Joel S. Emer. 2017. Efficient Processing of Deep Neural Networks: A Tutorial and Survey. In *Proceedings of the IEEE*, Vol. 105. 2295–2329. <https://doi.org/10.1109/JPROC.2017.2761740> Canonical DNN accelerator taxonomy covering dataflows, data reuse, and energy efficiency.

[80] Philippe Tillet, H. T. Kung, and David Cox. 2019. Triton: An Intermediate Language and Compiler for Tiled Neural Network Computations. In *Proceedings of the 3rd ACM SIGPLAN International Workshop on Machine Learning and Programming Languages (MAPL)*. 10–19. <https://doi.org/10.1145/3315508.3329973> Tile-based GPU programming with heuristic performance model for kernel generation.

[81] Jan Treibig, Georg Hager, and Gerhard Wellein. 2010. LIKWID: A Lightweight Performance-Oriented Tool Suite for x86 Multicore Environments. In *Proceedings*

- 1625 *of the 39th International Conference on Parallel Processing Workshops (ICPPW)*. 207–
1626 216. <https://doi.org/10.1109/ICPPW.2010.38> Lightweight tools for thread/cache
1627 topology, affinity, and performance counter measurement.

[82] Adrian Tschandl, Mohamed Awad, et al. 2025. SwizzlePerf: Hardware-Aware
1628 LLMs for GPU Kernel Performance Optimization. *arXiv preprint arXiv:2508.20258* (2025). LLM-based spatial optimization for GPU kernels, up to 2.06x speedup
1629 via swizzling.

[83] Xizheng Wang, Qingxu Li, Yichi Xu, Gang Lu, Heyang Zhou, Sen Zhang, Yikai
1630 Zhu, Yang Liu, Pengcheng Zhang, Kun Qian, et al. 2025. SimAI: Unifying
1631 Architecture Design and Performance Tuning for Large-Scale LLM Training with
1632 Scalability and Precision. In *Proceedings of the 22nd USENIX Symposium on
1633 Networked Systems Design and Implementation (NSDI)*. 1–18. Full-stack LLM
1634 training simulator achieving 98.1% alignment with real-world results. Alibaba
1635 Cloud/Tsinghua..

[84] Zixian Wang et al. 2025. SynPerf: Synthesizing High-Performance GPU Kernels
1636 via Pipeline Decomposition. *arXiv preprint* (2025). Under review.

[85] Samuel Williams, Andrew Waterman, and David Patterson. 2009. Roofline: An
1637 Insightful Visual Performance Model for Multicore Architectures. *Commun.
1638 ACM* 52, 4 (2009), 65–76. <https://doi.org/10.1145/1498765.1498785>

[86] William Won, Taekyung Heo, Saeed Rashidi, Saeed Talati, Srinivas Srinivasan,
1639 and Tushar Krishna. 2023. ASTRA-sim2.0: Modeling Hierarchical Networks and
1640 Disaggregated Systems for Large-Model Training at Scale. In *Proceedings of the
1641 IEEE International Symposium on Performance Analysis of Systems and Software
1642 (ISPASS)*. 283–294. <https://doi.org/10.1109/ISPASS57527.2023.00035>

[87] Yannan Nellie Wu, Joel Emer, and Vivienne Sze. 2022. Sparseloop: An Analytical
1643 Approach to Sparse Tensor Accelerator Modeling. In *Proceedings of the 55th
1644 IEEE/ACM International Symposium on Microarchitecture (MICRO)*. 1–15. <https://doi.org/10.1109/MICRO56248.2022.00078>

[88] Gyeong-In Yu, Joo Seong Jeong, Geon-Woo Kim, Soojeong Kim, and Byung-
1645 Gon Chun. 2022. ORCA: A Distributed Serving System for Transformer-Based
1646

1647
1648
1649
1650
1651
1652
1653
1654
1655
1656
1657
1658
1659
1660
1661
1662
1663
1664
1665
1666
1667
1668
1669
1670
1671
1672
1673
1674
1675
1676
1677
1678
1679
1680
1681
1682
1683
1684
1685
1686
1687
1688
1689
1690
1691
1692
1693
1694
1695
1696
1697
1698
1699
1700
1701
1702
1703
1704
1705
1706
1707
1708
1709
1710
1711
1712
1713
1714
1715
1716
1717
1718
1719
1720
1721
1722
1723
1724
1725
1726
1727
1728
1729
1730
1731
1732
1733
1734
1735
1736
1737
1738
1739
1740